

Neuroimaging Techniques

Thien Thanh Dang-Vu
Pierre Maquet
Martin Desseilles

Normal sleep has been explored with functional brain imaging techniques to characterize the distribution of brain activity across and within the various stages of sleep. Positron emission tomography (PET) shows the neural distribution of compounds labeled with positron-emitting isotopes. For instance, PET using oxygen-15 labeled water ($H_2^{15}O$) gives an assessment of regional cerebral blood flow (rCBF), whereas PET with fluorodeoxyglucose (^{18}F -FDG) measures cerebral metabolic rate of glucose (CMRglu). PET has been repeatedly used in the past 2 decades to compare brain perfusion or glucose metabolism patterns between different stages of sleep and wakefulness. More recently, functional magnetic resonance imaging (fMRI) has also been used to study brain activity during sleep. This technique measures the variations in brain perfusion related to neural activity by assessing the blood oxygen level-dependent (BOLD) signal. The latter relies on the relative decrease in deoxy-hemoglobin concentration that follows the local increase in cerebral blood flow in an activated brain area. Although improvements have been made in the spatial resolution of PET, fMRI still benefits from a superior temporal resolution, which has allowed investigators to assess with fMRI brain activations related to specific neural oscillations within sleep stages and thus to characterize the neural correlates of sleep microarchitecture.

Sleep disorders have also been subject to a variety of neuroimaging studies, which have brought important insight into the pathophysiological characteristics of these disorders. Various imaging modalities have been used. They include neuroanatomical studies using magnetic resonance imaging (MRI) to analyze changes in brain structure with voxel-based morphometry (VBM), white matter changes with diffusion tensor imaging (DTI), or neuronal integrity with proton magnetic resonance spectroscopy (1H -MRS). Transcranial sonography (TCS) is used to detect local iron content and signs of neurodegeneration in brainstem structures. Functional neuroimaging studies involve PET or fMRI, as described earlier, but also single-photon emission computed tomography (SPECT). The latter shows the neural distribution of a gamma-emitting radioisotope usually attached to a particular radioligand with specific chemical binding properties. For example, SPECT with Technetium ^{99m}Tc ethyl cysteinate dimer (^{99m}Tc ECD) or

^{99m}Tc hexamethylpropyleneamine oxime (^{99m}Tc -HMPAO) evaluates the distribution of brain perfusion. Functional neuroimaging studies in sleep disorders have assessed brain responses throughout the sleep-wake cycle (during wakefulness in most of the cases) or in association with symptomatic events. Finally, SPECT and PET were also coupled with specific radioligands to evaluate regional neurotransmitter function, particularly for dopamine (DA).

Among sleep disorders that have been assessed with neuroimaging studies are obstructive sleep apnea (OSA), narcolepsy, restless legs syndrome (RLS), often associated with periodic limb movements (PLM) in sleep, parasomnias taking place either during rapid eye movement (REM) sleep (REM sleep behavior disorder [RBD]) or non-REM sleep (such as sleepwalking), and insomnia. A summary of brain imaging findings and representative figures will be provided for each of these clinical conditions.

It should be emphasized that acquiring neuroimaging data in patients with sleep disorders constitutes a technical challenge. In many of these disorders, the occurrence of movements—usually unpredictable—during image acquisition is likely to produce artifacts for both structural and functional procedures. Techniques such as SPECT, for instance, allow scan acquisition to be performed well after the radiolabeled compound has been injected during the period of interest, thus reducing the interference of movements with the imaging procedure.

Normal Sleep

PET studies demonstrated a global decrease of CMRglu (>40%) during non-REM sleep as compared to wakefulness. At the regional level, mostly decreases of CMRglu and rCBF were observed during non-REM sleep, in various subcortical structures and associative cortical areas. REM sleep, on the other hand, displayed a global CMRglu as high as during wakefulness. Locally, increases and decreases of CMRglu and rCBF were reported in areas responsible for the generation of REM sleep and some important characteristics of dreams. Beyond sleep stages, fMRI studies described neural responses associated with brain oscillations of sleep: spindles and slow waves during non-REM sleep, and pontogeniculo-occipital waves during REM sleep. Besides refining

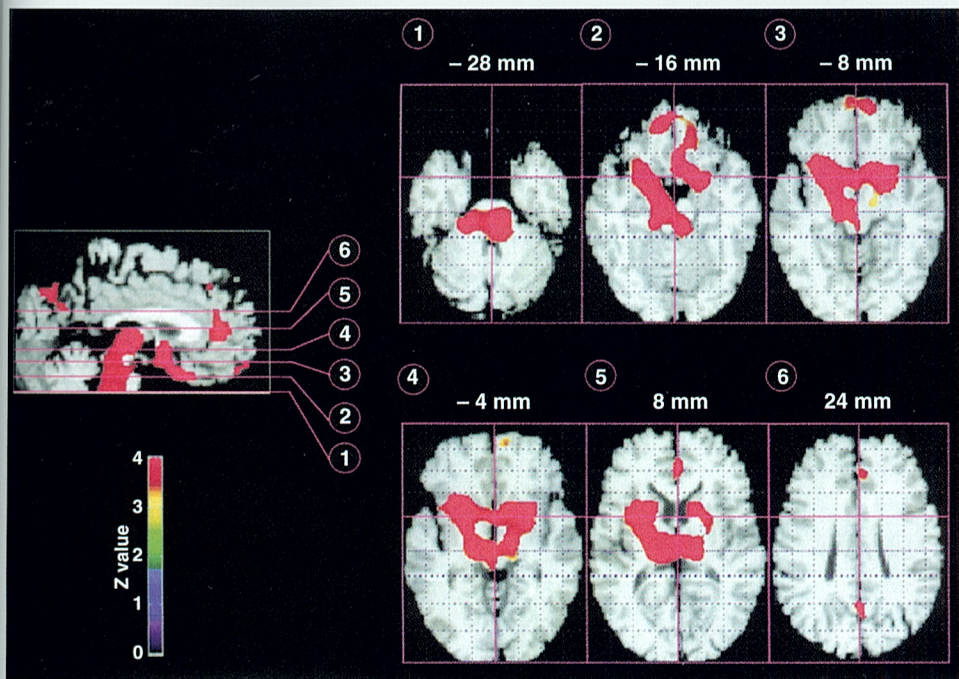


FIGURE 13.1 Functional neuroanatomy of normal human non-rapid eye movement (non-REM) sleep ($H_2^{15}O$ positron emission tomography). Brain areas in which regional cerebral blood flow decreases during non-REM sleep as compared to wakefulness and REM sleep. Image sections are displayed on different levels of the z-axis as indicated at the top of each image. The color scale indicates the range of Z values for the activated voxels, superimposed on a canonical T1-weighted magnetic resonance image. Displayed voxels are significant at $P < .05$ after correction for multiple comparisons. (Modified from Maquet P, Degueldre C, Delfiore G, et al. *Functional neuroanatomy of human slow wave sleep*. *J Neurosci*. 1997;17:2807-2812 with permission.)

the characterization of sleep functional neuroanatomy, fMRI data also demonstrated that non-REM sleep is not merely a passive state of brain deactivation, by showing enhanced brain responses associated with spindles and slow waves.

Non-REM Sleep

At the subcortical level, localized decreases of rCBF during non-REM sleep, as compared to wakefulness and REM sleep, were observed in the brainstem, thalamus, basal ganglia, and basal forebrain.¹ These structures include groups of neurons critical for the modulation of arousal and the generation of spontaneous neural oscillations of sleep. At the cortical level, although rCBF in primary cortices remained relatively preserved, decreases were located in several associative areas: (medial) prefrontal cortex, anterior and posterior cingulate gyrus, and precuneus. These areas are highly active in wakefulness, during which they are involved in complex cognitive processes and also participate in the modulation of non-REM sleep oscillations (see later). A representation of these PET results on non-REM sleep is provided in Figure 13.1.

Within non-REM sleep, fMRI studies reported brain activations associated with the major neural rhythms that define this sleep stage: spindles and slow waves. Spindles—prominent during stage N2—were correlated with increased brain responses in the lateral and posterior aspects of the thalamus, in agreement with the central role of several thalamic nuclei (reticular thalamic and thalamocortical neurons) in the generation of spindles.² Spindles were also associated with activation of specific paralimbic (anterior cingulate cortex, insula) and neocortical (superior temporal gyrus) areas. The hypothesis of two spindle subtypes—slow (11 to 13 Hz) and fast (13 to 15 Hz)—with distinct neural correlates was also explored with fMRI. It was observed that slow spindles exhibited a network very close to the "total" spindle one. In contrast, fast spindles were associated with a

more diffuse cortical activation extending to somatosensory areas and mid-cingulate cortex. These neural correlates of sleep spindles with fMRI are shown in Figure 13.2. Slow waves, on the other hand, were associated with enhanced brain responses in inferior and medial aspects of the prefrontal cortex, a major site for slow wave initiation as corroborated by electrophysiological data. Other activations correlated with slow waves were located in parahippocampal gyrus, precuneus, posterior cingulate cortex, cerebellum, and brainstem.³ The neural correlates of sleep slow waves are summarized in Figure 13.3. Altogether these fMRI studies have identified brain regions involved in the generation, propagation, or modulation of non-REM sleep oscillations.

REM Sleep and Dreaming

The brain imaging knowledge about human dreaming derives from the neurobiological study of REM sleep, during which dreams are prominent. Brain activity during REM sleep—as consistently demonstrated by PET studies—is dominated by increased rCBF in the pons, thalamus, temporo-occipital, and limbic/paralimbic areas (including amygdala, hippocampal formation, and anterior cingulate cortex), along with a relatively decreased rCBF in dorsolateral prefrontal and inferior parietal cortices. Of note, these results are in good agreement with animal neurophysiological data on REM sleep generation, in particular with ponto-geniculo-occipital waves. The existence of these rhythms, initially described from electrophysiological recordings in cats, is strongly suggested in humans by both PET and fMRI studies of REM sleep.

Combined with neuropsychological findings in brain-damaged patients, those patterns might also explain several hallmarks of dreaming experience that are found in dream reports after awakening from REM sleep.⁴ For example, the increased activity in the amygdala is consistent with the predominance of threat-related emotions in dreams. Temporo-occipital increased activity is in keeping with

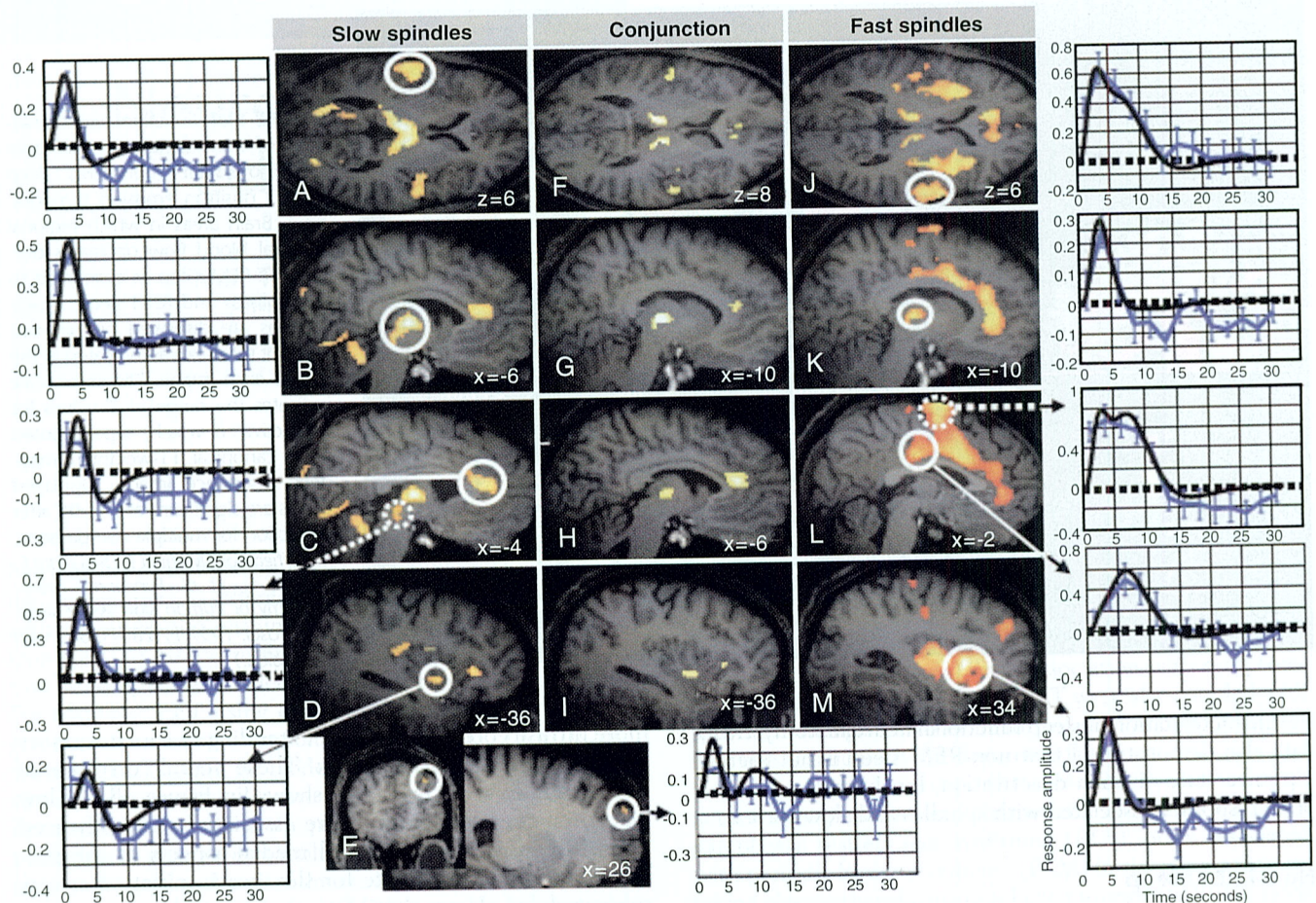


FIGURE 13.2 Functional neuroanatomy of sleep spindles (functional magnetic resonance imaging). Brain responses associated with all sleep spindles (i.e., slow and fast; center panels, F to I), slow spindles (left panels, A to E), and fast spindles (right panels, J to M), as compared to the baseline brain activity of non-REM sleep. Activations were significant at $P < .05$, corrected for multiple comparisons. The side panels show the time course (in seconds) of fitted response amplitudes (in arbitrary units) during spindles in the corresponding circled brain area. All responses consisted of regional increases of brain activity. (Modified from Schabus M, Dang-Vu TT, Albouy G, et al. Hemodynamic cerebral correlates of sleep spindles during human non-rapid eye movement sleep. *Proc Natl Acad Sci U S A.* 2007;104:13164-13169. Copyright 2007 National Academy of Sciences, U.S.A.)

visual dream imagery, which constitutes most of the sensorial experiment while dreaming. Also, prefrontal deactivation is evocative of the alteration in time perception, the lack of orientational stability, the delusional belief of being awake, the fragmented episodic memory recall, and the decrease in volitional control experienced in dreams. Finally, inferior parietal deactivation might contribute to the lack of distinction between first- and third-person perspectives, which is a core characteristic of the dream scenario. A summary of the neural correlates of REM sleep and dreaming is provided in Figure 13.4.

Obstructive Sleep Apnea

Neuroimaging studies have particularly addressed the neuropsychological damages induced by OSA. Structural alterations were found in the prefrontal cortex, hippocampal and parietal cortex in OSA patients before treatment, compared to controls. In these regions MRI using VBM found decreases of gray matter.⁵ Several of those abnormal patterns were, however, reversible under continuous positive

airway pressure (CPAP) treatment for 3 months. Structural changes were paralleled by impairments in various cognitive functions, which were improved after CPAP. Interestingly, posttreatment improvements in neuropsychological scores were correlated with posttreatment increases in gray matter, particularly in the hippocampus (Fig. 13.5).

Although the fundamental pathophysiological mechanisms are not fully understood, a central dysregulation of the autonomic nervous system might participate in these processes. For instance, during respiratory maneuvers (Valsalva), altered fMRI signals were shown in OSA patients compared to controls. These abnormal activations were located in the cerebellar cortex and deep nuclei; superior frontal, precentral, cingulate, inferior parietal, superior temporal, and insular cortices; hippocampus; and midbrain. These data suggest a dysfunction of neural structures integrating afferent airway signals with autonomic and somatic responses.⁶

It is important to notice that peripheral factors might confound the deficits observed in studies focused on OSA patients, including, for example, exaggerated body mass

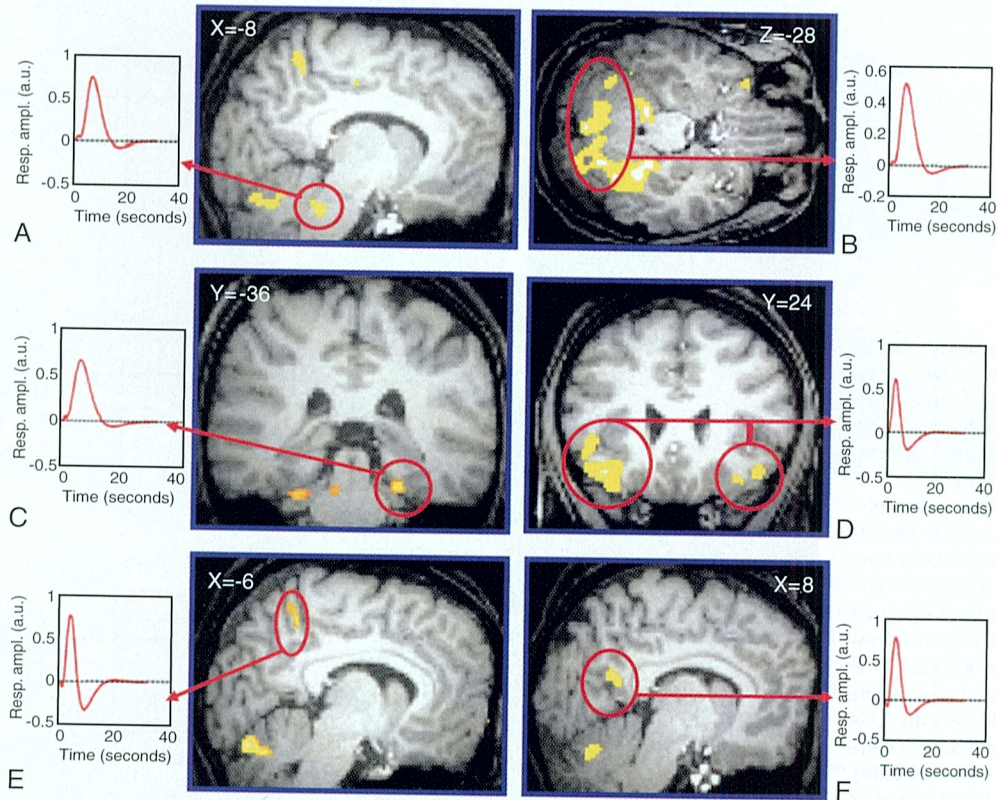


FIGURE 13.3 Functional neuroanatomy of sleep slow waves (functional magnetic resonance imaging). Brain responses associated with slow waves, as compared to the baseline brain activity of non-REM sleep. Brain responses were significant at $P < .05$, corrected for multiple comparisons. Activations were located in the pons (A), cerebellum (B), parahippocampal gyrus (C), inferior frontal gyrus (D), precuneus (E), and posterior cingulate gyrus (F). The *side panels* show the time course (in seconds) of fitted response amplitudes (in arbitrary units) during slow waves in the corresponding *circled* brain area. All responses consisted of regional increases of brain activity. (Modified from Dang-Vu TT, Schabus M, Desseilles M, et al. Spontaneous neural activity during human slow wave sleep. *Proc Natl Acad Sci U S A*. 2008;105:15160-15165. Copyright 2008 National Academy of Sciences, U.S.A.)

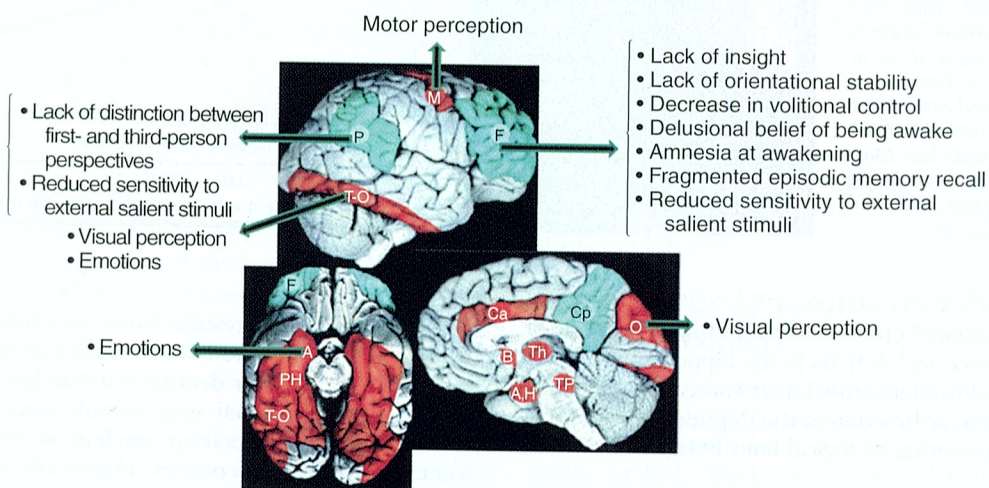


FIGURE 13.4 Functional neuroanatomy of rapid eye movement (REM) sleep and dreaming (positron emission tomography). Schematic representation of the relative decreases (in blue) and increases (in red) in regional cerebral blood flow or cerebral metabolic rate of glucose associated with REM sleep. Arrows show the proposed relationships between several dreaming features and cerebral regions associated with REM sleep. The *upper panel* displays a lateral view; the *right lower panel* displays a medial view; the *left lower panel* displays a ventral view. A, Amygdala; B, basal forebrain; Ca, anterior cingulate gyrus; Cp, posterior cingulate gyrus and precuneus; F, prefrontal cortex (middle, inferior, and orbitofrontal cortices); H, hypothalamus; M, motor cortex; O, occipital-lateral cortex; P, parietal cortex (inferior parietal lobule); PH, parahippocampal gyrus; Th, thalamus; T-O, temporo-occipital extrastriate cortex; TP, pontine tegmentum. (Modified from Schwartz S, Maquet P. Sleep imaging and the neuro-psychological assessment of dreams. *Trends Cogn Sci*. 2002;6:23-30. Copyright 2002, with permission from Elsevier.)

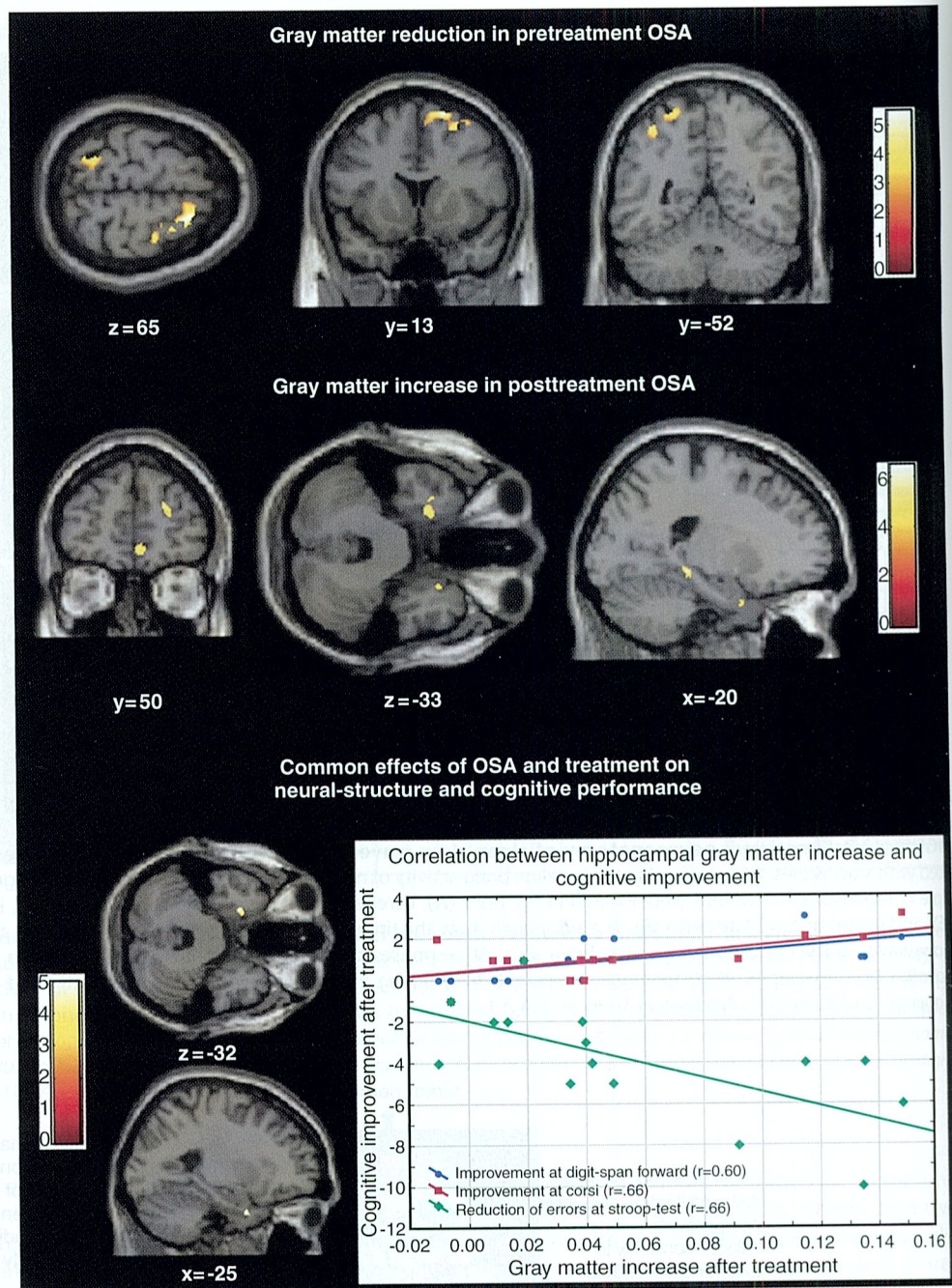


FIGURE 13.5 Structural brain changes in obstructive sleep apnea (OSA) before and after continuous positive airway pressure treatment (voxel-based morphometry). *Top row*, Regions showing a gray matter volume decrease in untreated patients with OSA compared with control subjects ($P < .05$ corrected for multiple comparisons based on cluster extent). *Middle row*, Regions showing a gray matter increase after treatment, compared to before treatment, in patients with OSA ($P < .05$ corrected for multiple comparisons based on cluster extent). *Bottom row*, Left hippocampal entorhinal cortex showing both a gray matter reduction before treatment and a gray matter increase after treatment ($P < .001$ uncorrected, based on a priori hypotheses) and the correlation between gray matter volume increase in this region and cognitive improvement after treatment ($P < .05$ corrected for multiple comparisons with false discovery rate). (From Canessa N, Castronovo V, Cappa SF, et al. Obstructive sleep apnea: brain structural changes and neurocognitive function before and after treatment. *Am J Respir Crit Care Med*. 2011;183:1419-1426. Copyright 2011, with permission from the American Thoracic Society.)

index and motivational problems. Interestingly, overlaps of structural and functional deficits in the hippocampus, anterior cingulate, and frontal cortex (areas consistently showing abnormal structure or function in the depression literature) provide several potential biological links between OSA and mood disorders.

Narcolepsy

Neuroimaging studies in narcoleptic patients have been conducted using different modalities. These works globally concur regarding a dysfunction of the hypothalamus and related areas, in agreement with a deficiency of the hypothalamic system in narcolepsy.

Indeed, although results from structural imaging using VBM vary from one study to the other, at least two of them evidenced gray matter decreases in the hypothalamus (e.g., Fig. 13.6).⁷ Additional gray matter decreases were also observed in the cerebellum, nucleus accumbens, and prefrontal and temporal cortices. Hypothalamic abnormalities in narcolepsy have also been found in one ¹H-MRS study, showing a local decrease of *N*-acetyl aspartate/creatine + phosphocreatine in that structure, which might reflect either a local neuronal loss or a neuronal dysfunction.

With the exception of one ¹⁸F-FDG-PET study that found increased CMRglu particularly in the cingulate cortex, other functional neuroimaging studies of narcoleptic patients conducted during wakefulness with either ¹⁸F-FDG-PET or

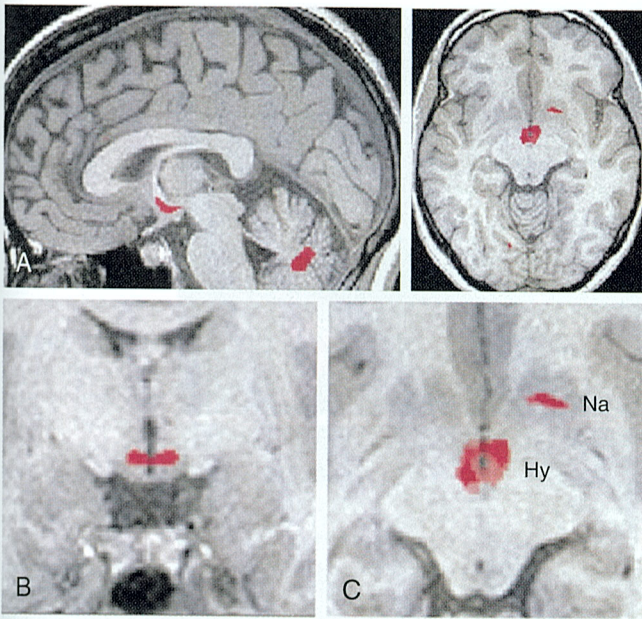


FIGURE 13.6 Structural brain changes in narcolepsy (voxel-based morphometry). A-C, Regions showing a decrease in gray matter in narcoleptic patients compared to controls are marked in red. These areas correspond to the hypothalamus (Hy), right nucleus accumbens (Na), and cerebellar vermis. Differences were significant at $P < .05$, corrected for multiple comparisons, and are superimposed on a normalized image of a healthy control subject. (Used with permission from *Nature Medicine*, copyright 2002. From Draganski B., Geisler P, Hajak G, et al. Hypothalamic gray matter changes in narcoleptic patients. *Nat Med.* 8[11]: 1186-1188.)

^{99m}Tc ECD SPECT evidenced a decreased metabolism or perfusion in hypothalamic and thalamic structures, thereby confirming a dysfunction of hypothalamus in these patients (Fig. 13.7). Additional hypoperfusions were found in the caudate nucleus and several cortical areas (prefrontal, post-central, parahippocampal, cingulate).⁸

Finally, a few functional neuroimaging studies have attempted to characterize the neural correlates of cataplexy in narcoleptic patients. Given the difficulty of triggering cataplexy in experimental conditions, such studies are very challenging. When comparing cataplectic episodes to a baseline waking condition in narcoleptic patients, increased perfusion was observed in the brainstem, thalamus, basal ganglia, limbic structures, and sensorimotor cortices. Perfusion decreases were found in the prefrontal and occipital cortices. When comparing cataplectic episodes in narcoleptic patients to wakefulness in healthy controls, increases in CMRglu were also found in the sensorimotor cortices, with additional hypermetabolism in the superior temporal gyrus.⁹ However, metabolic decreases were not evidenced in cortical areas, but in the hypothalamus, suggesting the involvement of this structure not only in the pathophysiology of narcolepsy in general, but also in the specific induction of cataplexy (Fig. 13.8). Instead of directly studying cataplexy, fMRI studies have assessed neural responses to emotional (humorous) pictures in narcolepsy, given that cataplexy is usually triggered by emotions and especially by positive stimuli such as jokes and laughter. Compared to controls, narcoleptic patients showed altered brain responses to humorous pictures in

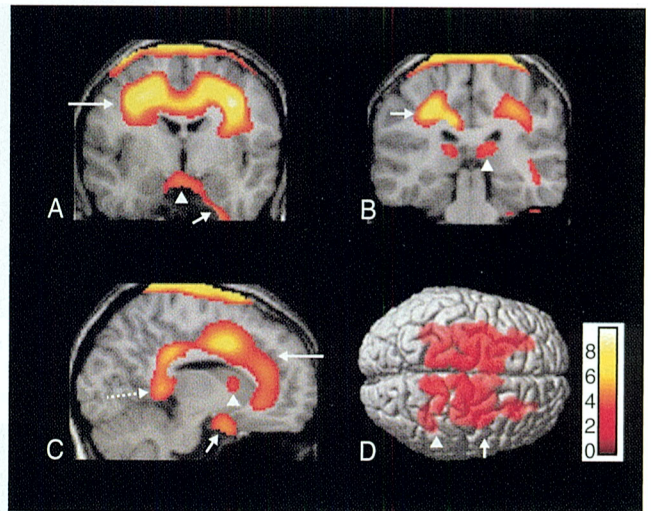


FIGURE 13.7 Functional brain changes in narcolepsy (technetium ^{99m}Tc ethyl cysteinate dimer single-photon emission computed tomography). Brain mapping of the regions where cerebral perfusion is decreased in narcoleptic patients compared to normal subjects. Results are overlaid on T1-weighted magnetic resonance imaging and are significant at false discovery rate (FDR)-corrected $P < .05$. A, Significant hypoperfusion was observed in bilateral anterior hypothalami (arrowhead) and in the right parahippocampal gyrus (short arrow). Bilateral cingulate gyri and white matter in bilateral middle frontal gyri (long arrow) showed decreased cerebral perfusion. B, Hypoperfusion was evident in bilateral posterior thalami (arrowhead) and in the white matter of the bilateral post-central and supramarginal gyri (short arrow). C, In the sagittal view of the right hemisphere, significant hypoperfusion was observed in the caudate nucleus (arrowhead), in the subcallosal gyrus (short arrow), the cingulate gyrus extending along the corpus callosum (long arrow), and in the parahippocampal gyrus (dotted arrow). D, Three-dimensional rendering showing decreased cerebral perfusion in bilateral paracentral areas (arrowhead) and superior/middle frontal gyri (short arrow). The frontal lobe is on the right and the occipital lobe on the left. (Reprinted from Yeon Joo E, Hong SB, Tae WS, et al. Cerebral perfusion abnormality in narcolepsy with cataplexy. *Neuroimage.* 2005;28:410-416. Copyright 2005, with permission from Elsevier.)

limbic structures, particularly in the amygdala, as well as in the hypothalamus, further suggesting a dysfunction of amygdalo-hypothalamic interactions in the central mechanisms of cataplexy.¹⁰

Restless Legs Syndrome and Periodic Limb Movements

Neuroimaging studies in RLS and PLM seem to demonstrate, although not consistently, a deficiency in the nigrostriatal DA system, both at presynaptic and postsynaptic levels. In RLS, MRI and ultrasound studies also show a central iron deficiency, located in the substantia nigra (SN). Other structures associated with these conditions are located in the brainstem, thalamus, red nucleus, sensorimotor cortical areas, and cerebellum, as evidenced by functional neuroimaging data. Altogether these results suggest that the DA dysfunction and central iron depletion in RLS ultimately affect brain structures responsible for sensorimotor control.

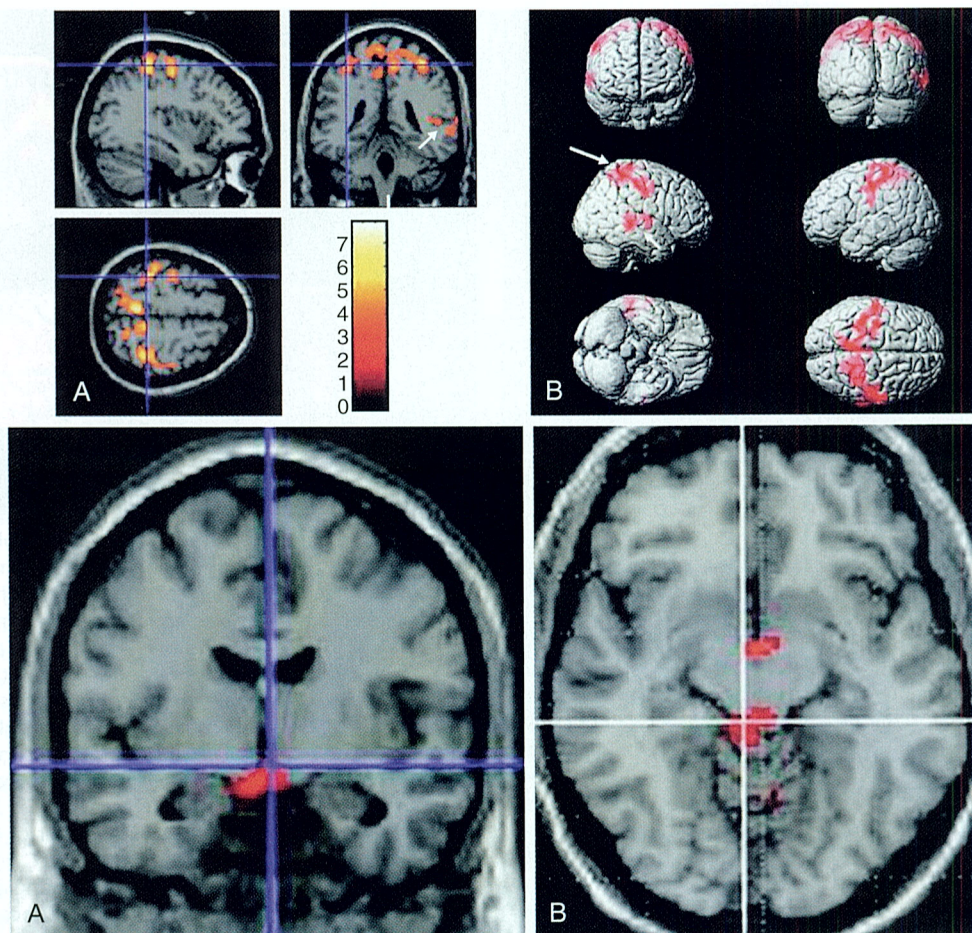


FIGURE 13.8 Functional brain changes associated with cataplexy in narcoleptic patients (^{18}F -fluorodeoxyglucose positron emission tomography). Brain mapping of the regions where significant changes in cerebral metabolic rate of glucose (CMRglu) were observed during cataplectic episodes in narcoleptic patients compared to normal subjects in the awake period. Results are overlaid on T1-weighted magnetic resonance imaging and were significant at false discovery rate (FDR)-corrected $P < .05$. *Upper panels*, Brain regions with increased CMRglu during cataplexy were located in the bilateral precentral and postcentral gyrus and primary somatosensory cortex (*long arrow*) and in the right superior temporal gyrus (*short arrow*), as shown on sagittal, coronal, and transversal views of the brain (A) and in the three-dimensional rendering (B). *Lower panels*, Decreased CMRglu during cataplexy was restricted to the hypothalamus, as shown on coronal (A) and transversal (B) sections of the brain. (Reprinted from Dauvilliers Y, Comte F, Bayard S, Carlander B, Zanca M, Touchon J. A brain PET study in patients with narcolepsy-cataplexy. *J Neurol Neurosurg Psychiatry*. 2010;81:344-348. Copyright 2010, with permission from BMJ Publishing Group.)

Restless Legs Syndrome

Structural abnormalities in idiopathic RLS, either with VBM or DTI, were quite inconsistent across studies. Whereas earlier studies found gray and white matter alterations in/around the thalamus and primary sensory-motor cortices, more recent studies found no neurostructural change. Using MRI with R_2' measurements sensitive to local iron content, several studies consistently found a decrease of iron concentration in the SN, which was correlated with RLS severity from clinical scales. More recent reports suggest that this iron decrease is particularly found in the pars compacta of the SN and can also be observed in other brain areas such as the thalamus and caudate nucleus. Iron brain concentration can also be assessed by TCS, because SN echogenicity is associated with local iron content. TCS studies have consistently shown a hypoecho-genicity of the SN in RLS patients, further confirming a reduction of iron concentration in this area (Fig. 13.9).¹¹

As for functional brain imaging, although no significant difference was found between patients and controls outside

the symptomatic period, a bilateral activation of the cerebellum and a contralateral activation of the thalamus was observed with fMRI during symptomatic periods of sensory leg discomfort¹² (Fig. 13.10). Functional MRI responses to a motor paradigm involving flexion and extension of both feet showed a higher activation of the dorsolateral prefrontal cortex in RLS patients compared to controls. Tonic electromyography, which was found inversely correlated with subjective sensory leg discomfort in RLS patients, was positively correlated with fMRI responses in sensorimotor cortical areas, cingulate gyrus, precuneus, and occipital cortex and negatively correlated in the cerebellum. Altogether these functional results suggest an involvement of thalamocortical sensorimotor pathways, as well as additional structures (including the cerebellum) in the pathophysiology of RLS.

Finally, SPECT and PET studies in association with various radiolabeled compounds were used to assess neurotransmission abnormalities, mostly in the nigrostriatal DA system. The results are quite inconsistent across studies.

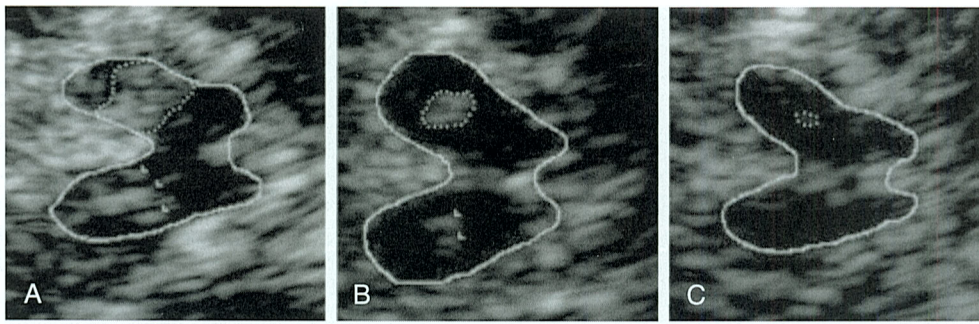


FIGURE 13.9 Decreased iron concentration in substantia nigra (SN) of restless legs syndrome (RLS) patients (transcranial sonography). Representative ultrasound images of the human mesencephalic brainstem. SN (encircled with *dotted line* on the side of insonation and marked contralaterally with *arrowheads*) appears hyperechogenic in the hypoechogenic brainstem area (*solid line*). **A**, Patient with Parkinson's disease (PD), showing SN hyperechogenicity (SN area $\geq .19$ cm² on one or both sides), which is typical for idiopathic PD. **B**, Healthy control, showing a regularly sized SN area of echogenicity. **C**, RLS patient, showing hypoechogenic SN (SN sum area of both sides ≤ 0.2 cm²); SN is often not delineable contralaterally. (From Godau J, Schweitzer KJ, Liepelt I, Gerloff C, Berg D. *Substantia nigra hypoechogenicity: definition and findings in restless legs syndrome*. *Mov Disord*. 2007;22:187-192. Copyright 2007, with permission from John Wiley and Sons.)

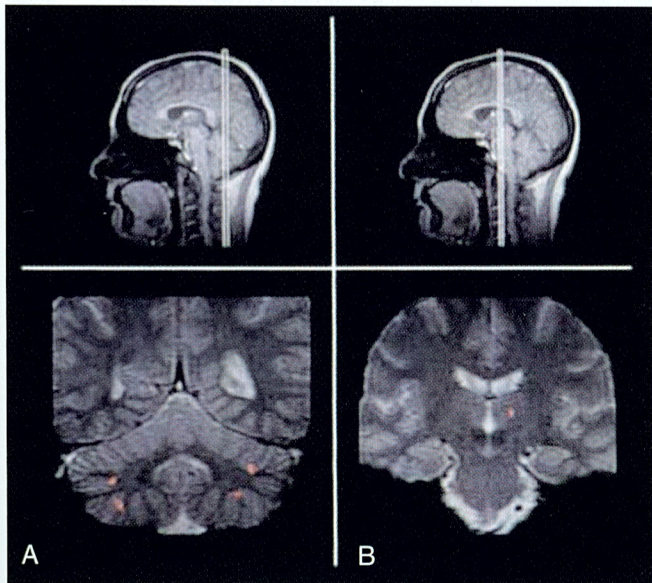


FIGURE 13.10 Functional brain changes in restless legs syndrome (RLS) (functional magnetic resonance imaging). Neural responses associated with sensory leg discomfort in a patient with idiopathic RLS. Activations are superimposed on two coronal T2-weighted magnetic resonance imaging sections, and the extents of activated areas were significant at $P < .05$ corrected for multiple comparisons. Activations were located in the cerebellum bilaterally (**A**) and in the contralateral thalamus (**B**). (From Bucher SF, Seelos KC, Oertel WH, Reiser M, Trenkwalder C. *Cerebral generators involved in the pathogenesis of the restless legs syndrome*. *Ann Neurol*. 1997;41:639-645. Copyright 1997, with permission from John Wiley and Sons.)

Some of the earlier reports tended to demonstrate the absence of significant change in DA neurotransmission. However, most recent articles found DA dysfunction both at the presynaptic (DA transporter) and postsynaptic (D₂ receptor) levels, mostly in the striatum.

Periodic Limb Movements

Because of their frequent association, RLS and PLM were usually considered together in neuroimaging studies. Only a few reports have assessed PLM more specifically.

In the fMRI study of Bucher et al,¹² RLS patients were also scanned during periods of sensory leg discomfort combined with PLM during wakefulness. This mixed condition resulted in the activation of the red nuclei and brainstem (Fig. 13.11), in addition to the thalamus and cerebellum, which suggested a subcortical origin for PLM.

As for DA neurotransmission, a negative correlation was found with SPECT between PLM number and striatal binding values for DA transporter in Parkinson's disease (PD) patients, suggesting that a presynaptic DA deficiency might be involved in PLM generation in PD. In addition, SPECT studies found a lower striatal D₂ receptor occupancy in PLM patients, which suggested that a DA dysfunction is also present at the postsynaptic level.

Parasomnias

Non-REM Parasomnias

The only available neuroimaging study in non-REM parasomnias is a single-case ^{99m}Tc ECD SPECT study of sleepwalking. Compared to quiet non-REM sleep, the sleepwalking episode was associated with increased perfusion in the posterior cingulate cortex and cerebellum. However, a decreased perfusion was observed in the frontoparietal associative cortices during the sleepwalking episode as compared to wakefulness in controls. Given that the posterior cingulate cortex, cerebellum, and frontoparietal associative cortices are deactivated during normal non-REM sleep (see earlier), these results were interpreted as reflecting a dissociated state, with a combination of non-REM sleep patterns (frontoparietal cortices), and persistent wakelike activities (cerebellum, posterior cingulate).

REM Sleep Behavior Disorder

Neuroimaging studies in RBD have mostly converged on two main conclusions. On the one hand, they have demonstrated alterations in the pons, supporting the involvement of pontine structures in the pathophysiology of RBD. On the other hand, they support the presence of degenerative changes in the SN, along with a presynaptic dysfunction of the DA nigrostriatal system in RBD. Altogether these

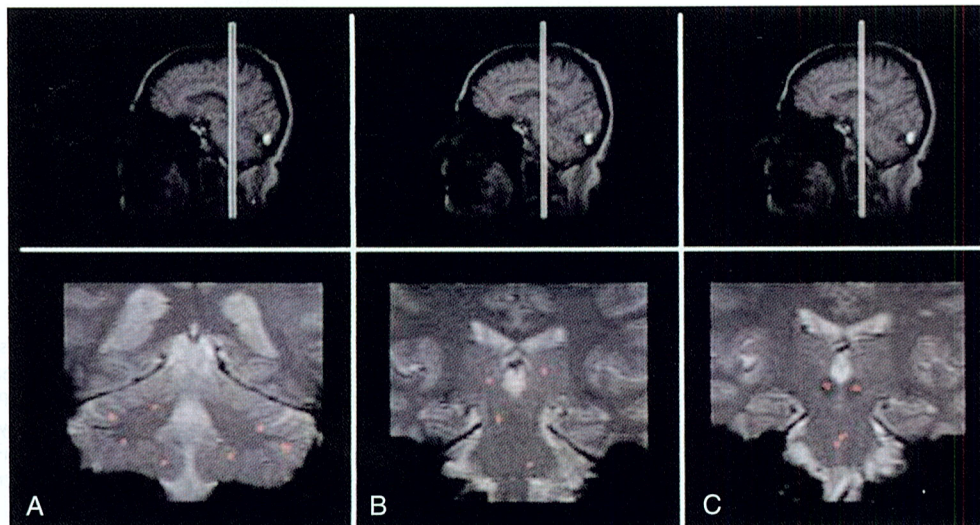


FIGURE 13.11 Functional brain changes associated with periodic limb movements (PLM) (functional magnetic resonance imaging). Neural responses associated with combined sensory leg discomfort and PLM during wakefulness in a patient with idiopathic restless legs syndrome (RLS). Activations are superimposed on three coronal T2-weighted magnetic resonance imaging sections, and the extents of activated areas were significant at $P < .05$ corrected for multiple comparisons. Activations were located in the bilateral cerebellum (A), thalamus (B), red nucleus (C), and the brainstem (pons and mesencephalon; B, C). (From Bucher SF, Seelos KC, Oertel WH, Reiser M, Trenkwalder C. Cerebral generators involved in the pathogenesis of the restless legs syndrome. *Ann Neurol.* 1997;41:639-645. Copyright 1997, with permission from John Wiley and Sons.)

findings are in line with the conception of RBD as an early stage of neurodegenerative disorders (in particular for synucleinopathies: PD, dementia with Lewy bodies, and multiple system atrophy).

Structural imaging found both white and gray matter changes in RBD (Fig. 13.12). DTI showed microstructural changes in multiple brain areas such as the internal capsule, the left superior temporal lobe, the right occipital lobe, the fornix, and the olfactory region. Most importantly, alterations were also found in the pons and midbrain tegmentum,¹³ in agreement with animal data and lesion studies in humans suggesting the involvement of specific nuclei of the pons in RBD, such as the sublateral dorsal nucleus. Interestingly, gray matter increases were detected with VBM in the hippocampus,¹³ a finding corroborated by functional studies (see later). However, no consistent change in brainstem structures was found with ¹H-MRS studies. Degenerative changes in the SN, reflected by increased local echogenicity with TCS, have been specifically explored in RBD patients. TCS studies demonstrated SN hyperechogenicity in a high proportion of RBD patients (36% to 42%). This pattern was found in an even higher proportion of PD patients (>50%), suggesting a continuum in SN degeneration from RBD to PD. Importantly, among RBD patients who would later evolve to a synucleinopathy, more than 60% had SN hyperechogenicity at baseline, which suggests that TCS might be helpful in identifying RBD patients at increased risk for the development of full-blown neurodegenerative disorders.

Functional brain imaging in RBD has used SPECT to assess the distribution of brain perfusion. Decreases of perfusion were observed during baseline wakefulness in the prefrontal and temporoparietal cortices, whereas hyperperfusion was present in the pons, putamen, and hippocampus (Fig. 13.13).¹⁴ Changes in the hippocampus and putamen are also characteristic of PD at the early stages

and are therefore in line with a continuum of pathophysiological modifications between RBD and PD. Preliminary data assessed functional changes during a behavioral episode of RBD in a single patient and found increased perfusion in the supplementary motor area as compared to wakefulness.

Finally, SPECT and PET studies also investigated nigrostriatal DA function in idiopathic RBD. At the presynaptic level, studies consistently found a decrease in DA transporter in the striatum of RBD patients compared to controls¹⁵ (Fig. 13.14). In particular, there was a decrease in DA transporter from controls to subclinical RBD (i.e., with loss of muscular atonia during REM sleep in polysomnography, but no behavioral episodes), from subclinical RBD to manifest RBD, and then from RBD to PD, in agreement with progressive neurodegenerative changes along these conditions. Furthermore, DA transporter striatal binding was also negatively correlated with the severity of REM atonia loss. In follow-up studies it was shown that reduced DA transporter binding at baseline was present in 75% of RBD patients who would later evolve to a synucleinopathy, underlining the potential interest of SPECT ligand studies in the risk assessment for neurodegenerative progression. In addition, serial SPECT studies showed a further decline over time of striatal binding, in line with a progressive nigrostriatal presynaptic DA dysfunction. As for postsynaptic DA function, no consistent modification in striatal D₂ receptor density was observed, demonstrating that DA dysfunction in RBD is restricted to presynaptic changes.

Insomnia

Functional imaging studies with PET showed that primary insomnia is characterized by a specific pattern of regional brain activity¹⁶ (Fig. 13.15). On the one hand, through the transition from waking to non-REM-sleep, there is a

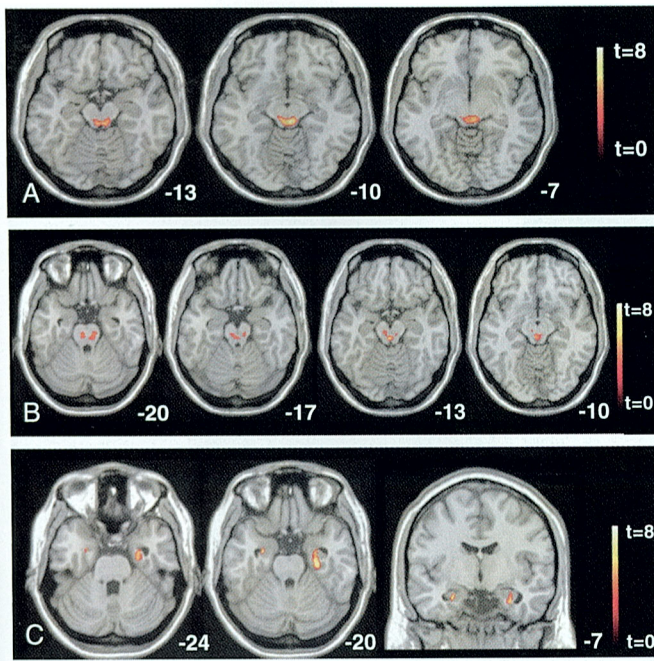


FIGURE 13.12 Structural brain changes in rapid eye movement sleep behavior disorder (RBD) (diffusion tensor imaging [DTI] and voxel-based morphometry [VBM]). Brain structural changes in idiopathic RBD patients compared to controls. Results are rendered onto a stereotactically normalized magnetic resonance imaging scan and were significant at $P < .001$ corrected for multiple comparisons. The number at the bottom right corner of each scan corresponds to the z coordinate (y coordinate for the last scan) in Talairach space. **A**, Areas of significant decreases of fractional anisotropy values (DTI), possibly corresponding to the periaqueductal gray matter in the mesencephalic tegmentum. **B**, Areas of significant increases of mean diffusivity values (DTI), possibly encompassing the sublateralodorsal nucleus and periaqueductal gray matter. **C**, Areas of significant increases of gray matter density values (VBM), located in the hippocampus bilaterally. (From Scherfler C, Frauscher B, Schocke M, et al. White and gray matter abnormalities in idiopathic rapid eye movement sleep behavior disorder: a diffusion-tensor imaging and voxel-based morphometry study. *Ann Neurol*. 2011;69:400-407. Copyright 2011, with permission from John Wiley and Sons.)

failure to diminish brain activity in the ascending reticular activating system, the medial prefrontal cortex, the limbic/paralimbic areas (including the amygdala, hippocampus, anterior cingulate and insular cortex), the thalamus, and the hypothalamus. On the other hand, during wakefulness there is a decrease of activity in the brainstem reticular formation, the thalamus and the hypothalamus, in the prefrontal, the left superior temporal, and the parietal and the occipital cortices. This specific distribution of brain

activity might relate to (1) specific impairments in daytime functioning (e.g., the reduced attentional abilities is consistent with the decrease of activity in the prefrontal cortex during wakefulness), (2) the hyperarousal hypothesis as a common pathway in the pathophysiology of insomnia (e.g., overall cortical hyperarousal characterized by an increase in electroencephalographic beta/gamma activity [14 to 35 / 35 to 45 Hz] at sleep onset and during non-REM sleep), and (3) the possibly overlapping pathophysiology with major depressive disorder, which has shown similarly impaired brain activity patterns (e.g., both conditions have impairments in limbic/paralimbic areas). Indeed, depression is the most common primary diagnosis in patients suffering from insomnia.

Structural imaging studies have also been performed in insomnia, particularly with VBM. Prefrontal alterations were also found, but mostly localized in the orbitofrontal region.¹⁷ Interestingly, gray matter density in this area was correlated with insomnia severity (Fig. 13. 16). Other data found decreases in hippocampal volumes in insomnia.

Structural alterations in insomnia might thus contribute to attentional deficits and cognitive impairments encountered in these patients.

Conclusion

Sleep and sleep disorders have been explored with a wide range of neuroimaging techniques, allowing detection of microstructural or functional changes associated with sleep stages, sleep oscillations, or sleep disorders. Besides the refinement of the physiology and pathophysiology of sleep, these techniques also show promising prospects for the diagnostic and prognostic evaluation of sleep disorders. Because a large proportion of neuroimaging studies in sleep medicine have been carried out during baseline wakefulness, further works are needed to describe the neural patterns underlying the disrupted sleep and behavioral manifestations characteristic of sleep disorders.

Acknowledgments

Thien Thanh Dang-Vu, Martin Desseilles, and Pierre Maquet were supported by the Fonds National de la Recherche Scientifique (Belgium). Thien Thanh Dang-Vu and Martin Desseilles were also supported by the Fonds Léon Fredericq (Belgium), the Belgian College of Neuropsychopharmacology and Biological Psychiatry, and the Canadian Institutes of Health Research. Thien Thanh Dang-Vu is currently supported by the Natural Sciences and Engineering Research Council of Canada, the Fonds de Recherche du Québec—Santé, the Sleep Research Society Foundation, and the Petro-Canada Young Innovators Awards Program.

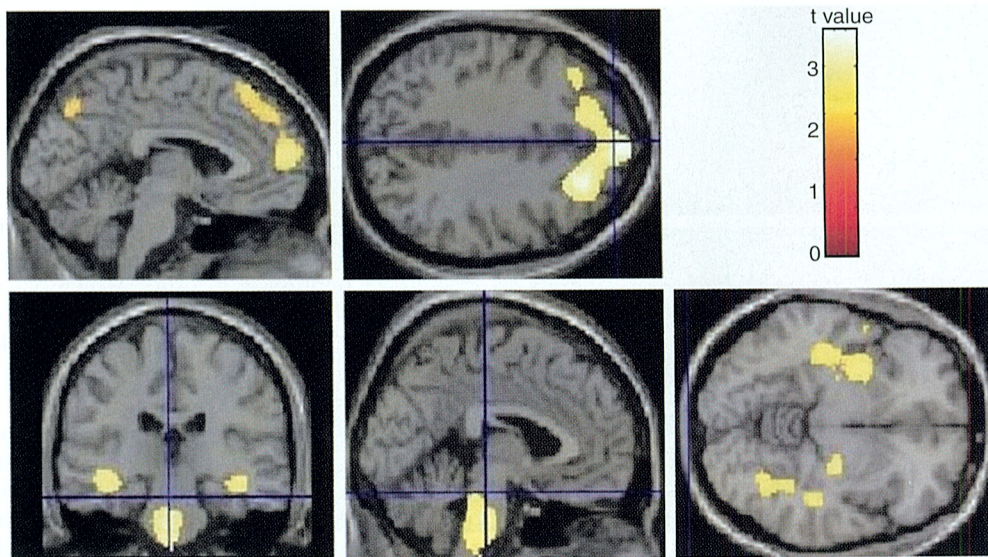


FIGURE 13.13 Functional brain changes in rapid eye movement sleep behavior disorder (RBD) (technetium ^{99m}Tc ethyl cysteinate dimer single-photon emission computed tomography). RBD is characterized by increases in regional cerebral blood flow in the pons, hippocampus, and putamen (*lower panels*) and decreases in medial frontal and parietal areas (*upper panels*) during wakefulness, as compared to healthy volunteers. Results are overlaid on T1-weighted magnetic resonance imaging and were significant at $P < .01$ for at least 50 contiguous voxels. (From Vendette M, Gagnon JF, Soucy JP, et al. Brain perfusion and markers of neurodegeneration in rapid eye movement sleep behavior disorder. *Mov Disord.* 2011;26:1717-1724. Copyright 2011, with permission from John Wiley and Sons.)

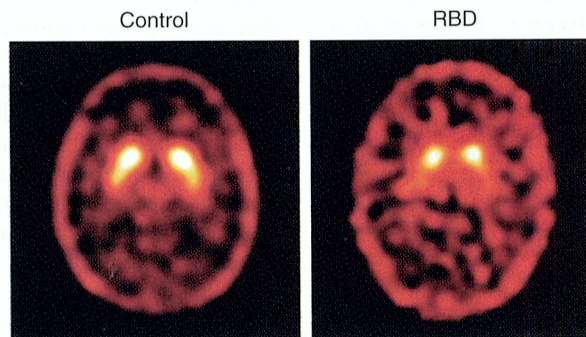


FIGURE 13.14 Dopaminergic function in rapid eye movement sleep behavior disorder (RBD) (^{123}I -(N)-(3-iodopropene-2-yl)-2beta-carbomethoxy-3beta-(4-chlorophenyl) tropane single-photon emission computed tomography). Dopamine transporter binding in one patient with RBD (*right*) and one control subject (*left*). Striatal binding was reduced on both sides in RBD, demonstrating a presynaptic dopamine deficit. Results were significant at $P < .05$. (From Eisensehr I, Linke R, Noachtar S, Schwarz J, Gildehaus FJ, Tatsch K. Reduced striatal dopamine transporters in idiopathic rapid eye movement sleep behaviour disorder: comparison with Parkinson's disease and controls. *Brain.* 2000;123[Pt 6]:1155-1160. Copyright 2000, with permission from Oxford University Press.)

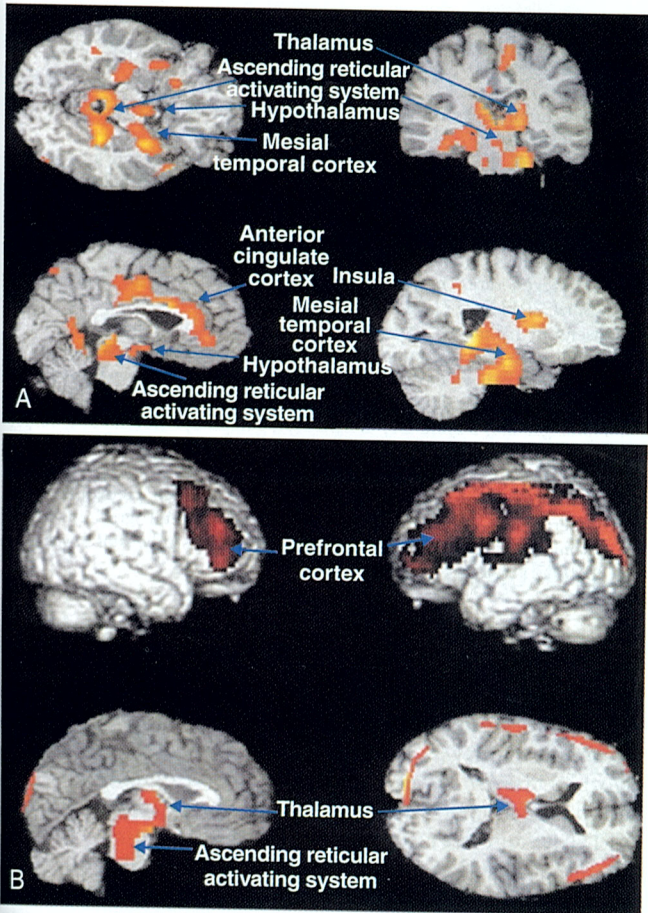


FIGURE 13.15 Functional brain changes in insomnia (^{18}F -fluorodeoxyglucose positron emission tomography). Distribution of brain glucose metabolism in patients with primary insomnia compared to healthy controls. Differences in all regions shown reached statistical significance at the level of $P < .05$, corrected. **A**, Brain structures that did not show decreased cerebral metabolic rate of glucose (CMRglu) from waking to non-rapid eye movement sleep in patients with insomnia. **B**, Brain structures where relative CMRglu while awake was higher in healthy subjects than in patients with insomnia. (From Nofzinger EA, Buysse DJ, Germain A, Price JC, Miewald JM, Kupfer DJ. Functional neuroimaging evidence for hyperarousal in insomnia. *Am J Psychiatry*. 2004;161:2126-2128. Copyright 2004, with permission from the American Psychiatric Association.)

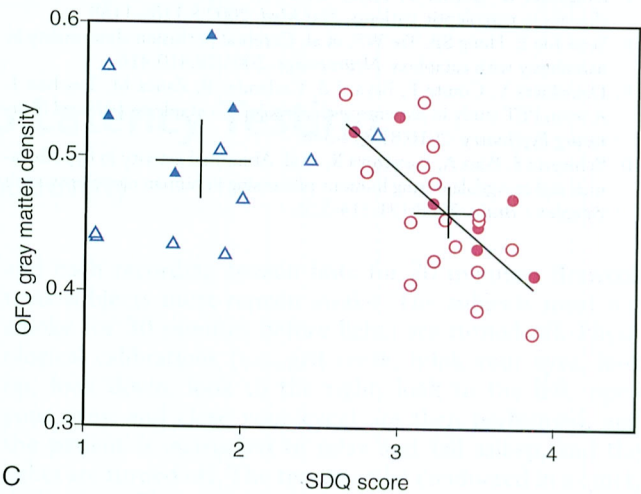
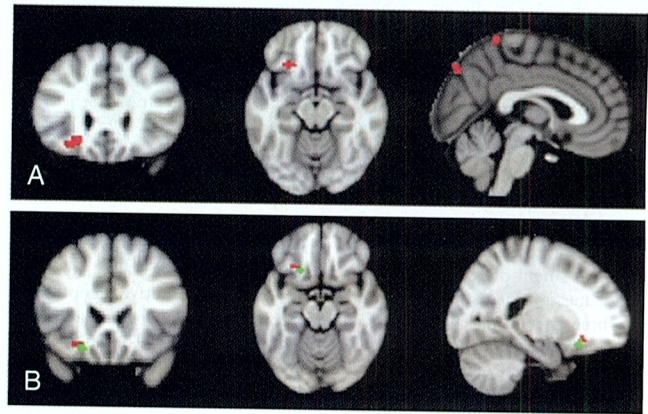


FIGURE 13.16 Structural brain changes in insomnia (voxel-based morphometry). Comparison of regional brain volumes between patients with chronic primary insomnia and healthy controls. **A**, Insomnia patients have a smaller gray matter volume than control subjects in areas (red voxels) of the left orbitofrontal cortex (OFC; coronal and axial slices, left and middle images, respectively) and precuneus (sagittal slice, right image). **B**, Regression analysis within the group of insomnia patients shows a strong negative relationship between gray matter volume in the orbitofrontal cortex and severity of insomnia measured by the Sleep Disorders Questionnaire (SDQ)—insomnia subscale (green voxels). **C**, Severity of insomnia is negatively correlated with left orbitofrontal gray matter density. Scatter plot with the SDQ insomnia subscale rating on the abscissa and the average value for gray matter density within the cluster, after controlling for age and total gray matter volume, on the ordinate. Crosshairs indicate group means \pm 95% confidence interval. Insomnia patients are shown as circles and control subjects as triangles (closed for men and open for women). (From Altena E, Vrenken H, Van Der Werf YD, van den Heuvel OA, Van Someren EJ. Reduced orbitofrontal and parietal gray matter in chronic insomnia: a voxel-based morphometric study. *Biol Psychiatry*. 2010;67:182-185. Copyright 2010, with permission from Elsevier.)

References

1. Maquet P, Degueldre C, Delfiore G, et al. Functional neuroanatomy of human slow wave sleep. *J Neurosci*. 1997;17:2807-2812.
2. Schabus M, Dang-Vu TT, Albouy G, et al. Hemodynamic cerebral correlates of sleep spindles during human non-rapid eye movement sleep. *Proc Natl Acad Sci U S A*. 2007;104:13164-13169.
3. Dang-Vu TT, Schabus M, Desseilles M, et al. Spontaneous neural activity during human slow wave sleep. *Proc Natl Acad Sci U S A*. 2008;105:15160-15165.
4. Schwartz S, Maquet P. Sleep imaging and the neuro-psychological assessment of dreams. *Trends Cogn Sci*. 2002;6:23-30.
5. Canessa N, Castronovo V, Cappa SF, et al. Obstructive sleep apnea: brain structural changes and neurocognitive function before and after treatment. *Am J Respir Crit Care Med*. 2011;183:1419-1426.
6. Henderson LA, Woo MA, Macey PM, et al. Neural responses during Valsalva maneuvers in obstructive sleep apnea syndrome. *J Appl Physiol*. 2003;94:1063-1074.
7. Draganski B, Geisler P, Hajak G, et al. Hypothalamic gray matter changes in narcoleptic patients. *Nat Med*. 2002;8:1186-1188.
8. Yeon Joo E, Hong SB, Tae WS, et al. Cerebral perfusion abnormality in narcolepsy with cataplexy. *Neuroimage*. 2005;28:410-416.
9. Dauvilliers Y, Comte F, Bayard S, Carlander B, Zanca M, Touchon J. A brain PET study in patients with narcolepsy-cataplexy. *J Neurol Neurosurg Psychiatry*. 2010;81:344-348.
10. Schwartz S, Ponz A, Poryazova R, et al. Abnormal activity in hypothalamus and amygdala during humour processing in human narcolepsy with cataplexy. *Brain*. 2008;131:514-522.
11. Godau J, Schweitzer KJ, Liepelt I, Gerloff C, Berg D. Substantia nigra hypochochogenicity: definition and findings in restless legs syndrome. *Mov Disord*. 2007;22:187-192.
12. Bucher SF, Seelos KC, Oertel WH, Reiser M, Trenkwalder C. Cerebral generators involved in the pathogenesis of the restless legs syndrome. *Ann Neurol*. 1997;41:639-645.
13. Scherfler C, Frauscher B, Schocke M, et al. White and gray matter abnormalities in idiopathic rapid eye movement sleep behavior disorder: a diffusion-tensor imaging and voxel-based morphometry study. *Ann Neurol*. 2011;69:400-407.
14. Vendette M, Gagnon JF, Soucy JP, et al. Brain perfusion and markers of neurodegeneration in rapid eye movement sleep behavior disorder. *Mov Disord*. 2011;26:1717-1724.
15. Eiseensehr I, Linke R, Noachtar S, Schwarz J, Gildehaus FJ, Tatsch K. Reduced striatal dopamine transporters in idiopathic rapid eye movement sleep behaviour disorder: comparison with Parkinson's disease and controls. *Brain*. 2000;123(Pt 6):1155-1160.
16. Nofzinger EA, Buysse DJ, Germain A, Price JC, Miewald JM, Kupfer DJ. Functional neuroimaging evidence for hyperarousal in insomnia. *Am J Psychiatry*. 2004;161:2126-2128.
17. Altena E, Vrenken H, Van Der Werf YD, van den Heuvel OA, Van Someren EJ. Reduced orbitofrontal and parietal gray matter in chronic insomnia: a voxel-based morphometric study. *Biol Psychiatry*. 2010;67:182-185.